Journal of Circuits, Systems, and Computers

SEMI-STATE MODELS FOR VLSI HAIR-CELL CIRCUITS*

LOUIZA SELLAMI
Electrical Engineering Department, US Naval Academy
105 Maryland Avenue, Annapolis, Maryland 21402, USA.
Microsystems Laboratory, Electrical Engineering Department
University of Maryland, College Park, Maryland 20742, USA.

KUAN WONG
Microsystems Laboratory, Electrical Engineering Department
University of Maryland, College Park, Maryland 20742, USA.

and

ROBERT W. NEWCOMB
Microsystems Laboratory, Electrical Engineering Department
University of Maryland, College Park, Maryland 20742, USA.
Electrical Engineering Department, POSTECH
Pohang 790-784, Republic of KOREA.

Received December 19, 1996
Revised March 27, 1997
Accepted May 2, 1997

Cochlea hair-cells act as neural interfaces of sound signals and, therefore, circuit representations are important to signal processing systems based upon characteristics of the ear. Here nonlinear semi-state equations for a bidirectional circuit representing a generic cochlea hair-cell are presented. The circuit can be specialized to inner or outer hair-cells depending upon the choice of circuit parameter values. Also developed are a canonical semi-state description for the hair-cell potassium and sodium channels, and circuits suitable for a transistorized hardware implementation. Circuit simulations are run with numerical data to correlate with the Howard-Hudspeth experiments.

Keywords: Semi-state Models, Hair-Cell Circuits, VLSI Circuits.

1. Introduction

Circuits which mimic the behavior of the cochlea are useful for determining properties of the ear from stimulated acoustic emissions, as well as for the design of ear-type systems.[1,2] Noninvasive stimulated emissions from the ear can presently determine damage to the basilar membrane. In the same way, stimulated emissions from the ear could possibly be used as a clinical tool to assess hair-cell damage if adequate models were available and, thus, could lead to the design of corrective aids to compensate for hearing loss.

The presence of nonlinearities and active behavior in the cochlea is supported by experimental data that show discrepancies between basilar membrane and neu-

*This paper was recommended by Nobuo Fujii, Guest Editor.

ral tuning. Two major categories of sources of cochlear nonlinearity have been suggested in the literature.[3,4] The first category finds its origins in the bounds on the motion of the basilar membrane and the cochlear fluids, and the second one resides in the mechano-electrical transduction process that occurs in the hair-cells: limits on the mechanical resonance of the stereociliary-tectorial structure and on the amplitude of electrical resonance of the hair-cell membrane. Experimental evidence has shown that this process, besides being an active one, is bidirectional and nonlinear.[3,4,5,6] It is believed that the bidirectional process of the hair-cells is the physical basis for a variety of phenomena observed in mammals, including Kemp echoes and spontaneous acoustic emissions.[1,2] Several hair-cell models have been proposed in the literature to attempt to replicate the firing behavior observed in hair-cell.[7,8,9] However, these models are computational and, thus, are different from ours in the sense that we focus on a hair-cell circuit to correlate with the Howard-Hudspeth experiments for interfacing with the scattering cochlea model.[4]

The scattering cochlea model developed previously is passive and linear.[10,11] But since experimental evidence shows that Kemp echo phenomena are active and nonlinear, it is important to incorporate nonlinearities and active behavior into the full model.[12] Toward this we treat here the nonlinearities and the active behavior due to the hair-cells and, therefore, as a first step, propose a nonlinear active bidirectional circuit model of a generic hair-cell, based on that of Weiss and Leong[13,14] and Secker, Searle, and Wilson[15] into which we incorporate biologically realistic models for sodium and potassium channels. The circuit model can be adapted to a specific type of hair-cell (inner or outer cochlea hair cells for instance) depending upon the choice of circuit parameter values. We then convert the equations describing the activities of the potassium and sodium channels to a canonical semi-state form from which we develop circuits appropriate for future VLSI implementation. Circuit simulations are run with numerical data to correlate with the Howard-Hudspeth measurements.

2. Hair-Cell-Type Circuits

The proposed active and nonlinear hair-cell circuit model, following from that of Weiss and Leong, is based on the mechano-electrical behavior of the hair-cells and embodies two parts: an electrical part and a mechanical part. The electrical part models the electrical activities of the hair-cell, namely the opening and closing of potassium and sodium channels, and transduction channels, specific to the hair-cells, that regulate the fluctuations of the membrane voltage, through the control of ion transport into the cell, and via which neural signals, encoding acoustical information, are transmitted to the brain.

The necessary element in causing both the depolarization and repolarization of the hair-cell is the voltage-gated sodium channels. However, the voltage-gated potassium channels also play an important role in increasing the rapidity of repolarization of the membrane. In the absence of any stimulation, the hair-cell is in its resting state, with the membrane potential being around $-61mv$. In this state the

sodium and potassium channels are closed. At the onset of a stimulus, the sodium channels open up instantaneously, allowing sodium ions to penetrate the cell and increase its potential. A fraction of a millisecond later, the potassium channels open up, allowing increased potassium flow outward, thus bringing down the membrane voltage. At the end of the depolarization-repolarization phase, the channels close back to their original status.

The opening and closing of these voltage-gated channels affect directly the permeability of the cell membrane to the potassium and sodium ions and, thus, the electrical conductance of the cell. Hence, these channels are modeled by the nonlinear conductances $G(\theta)$ and $G_{sh}(V_p)$ (given in Eqs. (1) and (2)) which we convert to current and voltage controlled nonlinear current sources for circuit realization purposes.

$$G(\theta) = G_0 + \frac{G_M}{2}\left[1 + \tanh\frac{\theta}{2\theta_0}\right]. \tag{1}$$

$$G_{sh}(V_p) = K\left[G_0 + \frac{G_M}{2}\left(1 + \tanh\frac{V_p}{2V_0}\right)\right]. \tag{2}$$

where G_0, G_M, θ_0, K, and V_0 are constant parameters estimated by curve fitting experimental data and θ represents the deflection angle of the hair-bundle. The slow process of the opening and closing of potassium channels is symbolically represented by the series path R_pC_p. The hair-cell membrane is represented by the nonideal capacitor C and its leakage resistance R and resting voltage V_c.

The mechanical part of the hair-cell concerns mainly the movement of the hair-bundle and its bidirectional coupling with the body of the cell. The hair-bundle is modeled by a second order mechanical system with an inertia J, a viscous drag B, and a compliance C_M, and the electro-mechanical feedback by a torque controlled by the membrane potential V_m. The mechanical system is then converted to an electrical equivalent circuit consisting of an RLC circuit in series with a nonlinear voltage controlled voltage source $T_R(V_m)$, which mimics the electro-mechanical feedback, and where now θ represents the electric charge across C_M. The results are summarized in Eqs. (3) and (4) which also describe the input-output (hair-bundle deflection-cell membrane voltage) characteristic.

$$T_F = -T_R(V_m) + J\frac{\partial^2\theta}{\partial t^2} + B\frac{\partial\theta}{\partial t} + \frac{\theta}{C_{MF}}. \tag{3}$$

$$T_R(V_m) = K'\left[\tanh\left(\frac{V_m + V_{off}}{V_{ref}}\right) - \frac{V_{off}}{V_{ref}}\right]. \tag{4}$$

where C_{MF} is the series equivalent of C_M and C_F and K', V_{off}, and V_{ref} are constants estimated by curve fitting experimental data.

By combining the circuit models for the electrical and mechanical parts of the hair cell, we obtain the circuit shown in Fig. 1, where T_F is a voltage source representing the stimulus torque applied to the hair-bundle. Because we are interested in reproducing the Howard-Hudspeth measurements, we add a capacitor C_F to account for the compliance of the glass fiber Howard and Hudspteh use in their experiment to drive the hair-bundle.[4]

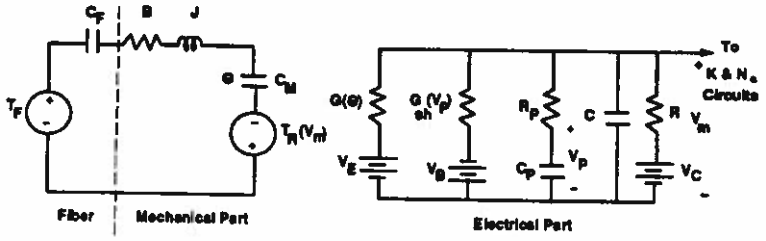

Fig. 1. The electrical equivalent nonlinear bidirectional model of a hair-cell with fiber excitation.

3. Semi-State Equations and Circuits for Hair-Cell Model

The canonical semi-state representation takes the form of the equations

$$E\frac{dx}{dt} = A(x,t) + Bu. \tag{5}$$

$$y = Cx. \tag{6}$$

where u, x, y are the input, semistate, and output vectors, B, C, E constant matrices (with E possibly singular), and $A(.,.)$ a possibly nonlinear function. These are very useful for VLSI design using current mode circuits. Consequently, we obtain such a representation for the nonlinear hair-cell-type structures considered here and represented by Fig. 1 with the addition of the refinements of Fig. 2 to include ion channels as mentioned below.

In the hair-cell circuit of Fig. 1 the slow process of the opening and closing of potassium and sodium channels is modeled by allowing the effective conductances of these channels to vary according to laws determined by Hartline[16] and given below as Eqs. (7) and (8)

$$G_i = \frac{G_{mi}}{1+\exp[-(V_m(t)-V_{oi})/\mu_i]} \quad i = Na, K. \tag{7}$$

where G_{mi}, V_{oi} and μ_i are constants associated with the basic sodium, $i = Na$, or

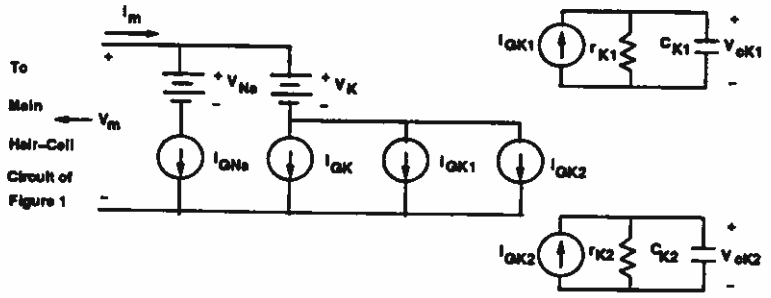

Fig. 2. Equivalent circuit for the hair-cell potassium and sodium channels semistate equations.

potassium, $i = K$, channels. Physically, G_{mi} is the maximum conductance, reached when all channels are open, V_{oi} a half-activation voltage and μ_i the channel characteristic voltage. In addition to the characterization in terms of voltage dependent conductances, there is the slow opening and closing of these channels which are modeled by the following differential equations due to Hartline.[16]

$$\tau_{Ki}\frac{dG_{Ki}}{dt} = \frac{G_{mKi}}{1+\exp[-(V_m(t)-V_{oi})/\mu_i]} - G_{Ki}. \tag{8}$$

for $i = 1,2$ and where τ_{K1} and τ_{K2} are the slow and fast time constants for these two channels.

To lead to transistorized hardware implementations for the hair-cell circuit, we interpret these laws in terms of a basic circuit (Fig. 2) for which canonical semistate equations are derived below, following a previous treatment.[17,18] With Fig. 2 in hand, we set the semistate vector for it as

$$x = [V_{cK1}, V_{cK2}, i_{GNa}, i_{GK}, i_{GK2}, i_{GK2}, V_m, i_m]^T. \tag{9}$$

and describe the dynamics by

$$\begin{bmatrix} \tau_{K1} & \cdot & \cdot & \cdot & \cdot & \cdot & \cdot & \cdot \\ \cdot & \tau_{K2} & \cdot & \cdot & \cdot & \cdot & \cdot & \cdot \\ \cdot & \cdot & \cdot & \cdot & \cdot & \cdot & \cdot & \cdot \\ \cdot & \cdot & \cdot & \cdot & \cdot & \cdot & \cdot & \cdot \\ \cdot & \cdot & \cdot & \cdot & \cdot & \cdot & \cdot & \cdot \\ \cdot & \cdot & \cdot & \cdot & \cdot & \cdot & \cdot & \cdot \\ \cdot & \cdot & \cdot & \cdot & \cdot & \cdot & \cdot & \cdot \\ \cdot & \cdot & \cdot & \cdot & \cdot & \cdot & \cdot & \cdot \end{bmatrix} \dot{x} \quad =$$

$$\begin{bmatrix} -1 & . & . & . & . & . & . & . \\ . & -1 & . & . & . & . & . & . \\ . & . & -1 & . & . & . & . & . \\ . & . & . & -1 & . & . & . & . \\ . & . & . & . & -1 & . & . & . \\ . & . & . & . & . & -1 & . & . \\ . & . & 1 & 1 & 1 & 1 & . & -1 \\ . & . & . & . & . & . & A_v & A_i \end{bmatrix} x +$$

$$\begin{bmatrix} G_{K1}(x_7) \\ G_{K2}(x_7) \\ G_{Na}(x_7)[x_7 - V_{Na}] \\ G_K(x_7)[x_7 - V_K] \\ x_1(x_7 - V_K) \\ x_2(x_7 - V_K) \\ 0 \\ 0 \end{bmatrix} + Bu. \tag{10}$$

Here the .'s inside the matrices represent 0 and the A_v and A_i depend on the choice of the input. Also, for compactness we have defined for (7)

$$G_j(V_m) = \frac{G_{MKj}}{1 + exp[-(V_m(t) - V_{0j})/\mu_j]}. \tag{11}$$

for $j = Na, K, K_1, K_2$ and where $V_{oK1} = V_{oK2} = V_{oK}$. $G_j(V_m)$ represents the current i_j for a 1Ω resistance r_j. Next we determine the matrices B and C for the two cases (admittance or impedance basis) below.

Case 1: $u = V_m, y = i_m$. By inspection we get

$$\begin{aligned} B &= [0,0,0,0,0,0,1,0]^T, \quad A_v = -1 \\ C &= [0,0,0,0,0,0,0,1], \quad A_i = 0. \end{aligned} \tag{12}$$

Case 2: $u = i_m, y = V_m$. In this case

$$\begin{aligned} B &= [0,0,0,0,0,0,0,1]^T, \quad A_v = 0 \\ C &= [0,0,0,0,0,0,1,0], \quad A_i = -1. \end{aligned} \tag{13}$$

For a complete semi-state description of the hair-cell circuit of Fig. 1, we first adjoin to the semi-state x the variables $x_9 = V_p$, $x_{10} = \theta$, and $x_{11} = \dot{\theta}$. Then in Eq. (10), we replace u by x_7 for case 1 and by x_8 for case 2, and set $T_F = u$ in Eq. (3).

Finally, we add to Eq. (10) Eqs. (1)-(4) and the equations for the currents through capacitors C and C_p. These latter two equations are obtained through Kirchhoff's current law as follows:

$$\begin{aligned} C\frac{dV_m}{dt} &= -i_m - G_p(V_m - V_p) - \\ &\quad G(V_m - V_c) - G_{sh}(V_p)(V_m - V_B) - \\ &\quad G(\theta)(V_m - V_E). \end{aligned} \tag{14}$$

$$C_p\frac{dV_p}{dt} = -G_p(V_m - V_p). \tag{15}$$

where $G_p = 1/R_p$ and $G = 1/R$.

4. Simulation and Results

To test the circuit models we perform a Spice simulation of the nonlinear bidirectional circuit of Fig. 1 incorporating those of Fig. 2 to include potassium and sodium channels, with the circuit components being estimated from data of the Howard-Hudspeth experiments.[1] The resulting Spice circuit is shown in Fig. 3. Because the mechanical part is converted from recti-linear to rotational, on the one hand, and from mechanical to electrical, on the other hand, the resulting circuit is scaled down to bring the values of capacitances C_F and C_M to reasonable simulation values. Also, the initial conditions across the capacitors are set up so that the resting potential of the cell is -61 mv. We excite the circuit with a voltage pulse of magnitude 4.8 mv and width 25 ms, simulating the torque T_F, and measure the membrane potential V_m and the voltage V_{CM} across C_M. The latter is proportional to θ which represents the deflection of the stereocilia of the hair-cell. Here we give the parameter and circuit component values used in the simulation.

For the mechanical part:

$$\begin{array}{ll} C_F = 8.307 & B = 63.94510^{-5} \\ J = 2.87510^{-15} & C_M = 2376 \\ K' = -2.37710^{2} & V_{ref} = 10mV \\ V_{off} = -10mV. & \end{array} \tag{16}$$

For the electrical part:

$$\begin{array}{ll} V_E = 100mV & G_0 = 10^{-6} \\ G_M = 10^{-5} & \theta_0 = 210^{-2} \\ V_B = 100mV & K = 13 \\ V_0 = 25mV & C_p = .1\mu F \\ R_p = 20K\Omega & C = 0.005\mu F \\ R = 5M\Omega & V_c = -61mV. \end{array} \tag{17}$$

For the semistate circuits:

$$
\begin{array}{ll}
V_{Na} = 40mV & V_K = -90mV \\
C_{K1} = .8\mu F & C_{K2} = 1\mu F \\
r_{K1} = 12.5K\Omega & r_{K2} = 1M\Omega \\
\mu_K = 5mV & \mu_{Na} = 5mV \\
V_{oK} = -20mV & V_{oNa} = -20mV \\
G_{mK} = 510^{-5} & G_{mNa} = 510^{-5} \\
G_{mK1} = 0.3510^{-6} & G_{mK2} = 0.3510^{-6}.
\end{array}
\tag{18}
$$

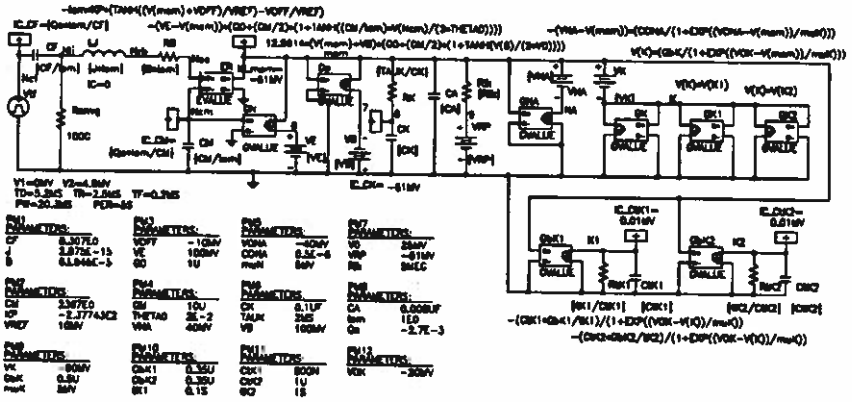

Fig. 3. The SPICE circuit.

As shown in Fig. 4 and Fig. 5 the results obtained reproduce the waveforms for the membrane potential recorded by Howard and Hudspeth in their shape and order of magnitude. Note that in the Howard-Hudspeth case as well as in ours the membrane potential becomes even more negative than the original resting potential for a short period of time. This is caused by the fact that many potassium channels remain open for several milliseconds after the repolarization process of the membrane is complete. This allows excess potassium ions to diffuse out of the cell, leaving a deficit of positive charges on the inside, which means a more negative membrane potential. This phenomenon has been observed in hair-cells as well as in other cells of the body.

5. Discussion

In this paper we have presented a nonlinear bidirectional hair-cell circuit and developed a set of canonical semi-state equations and circuits for its potassium and

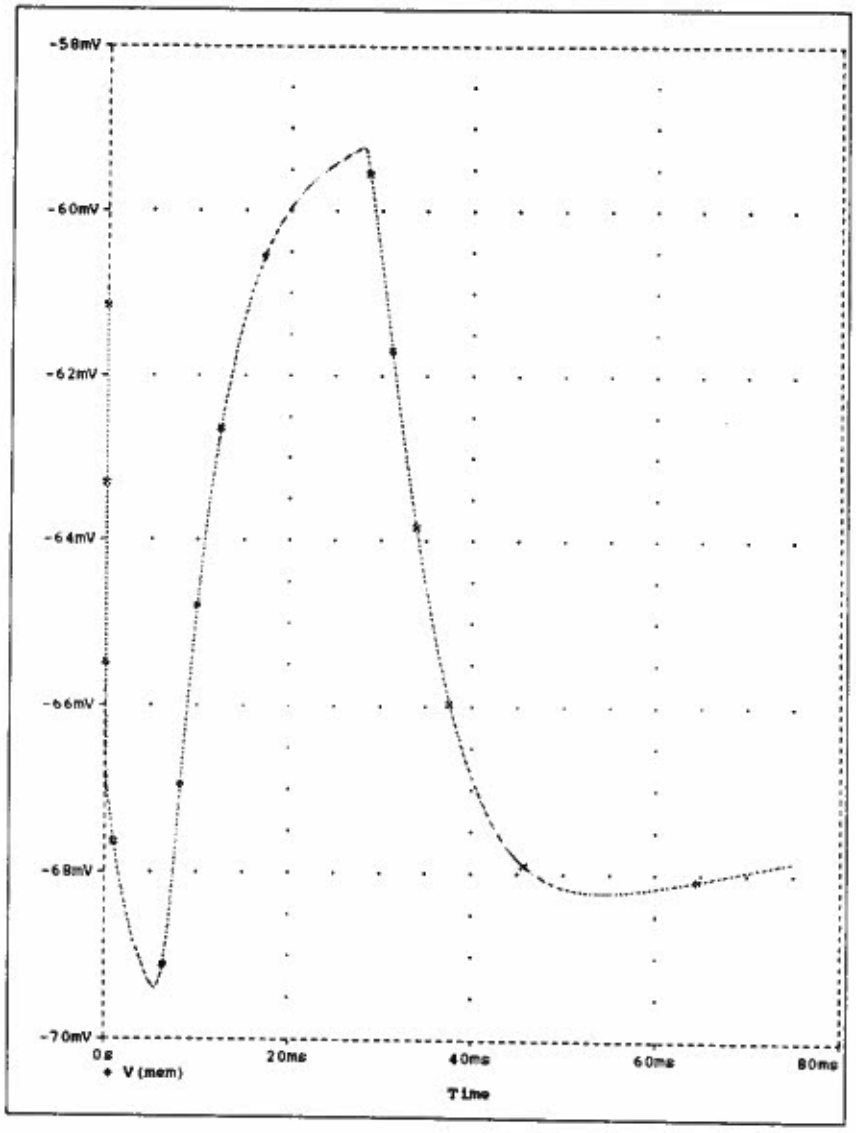

Fig. 4. The hair-cell membrane potential V_m.

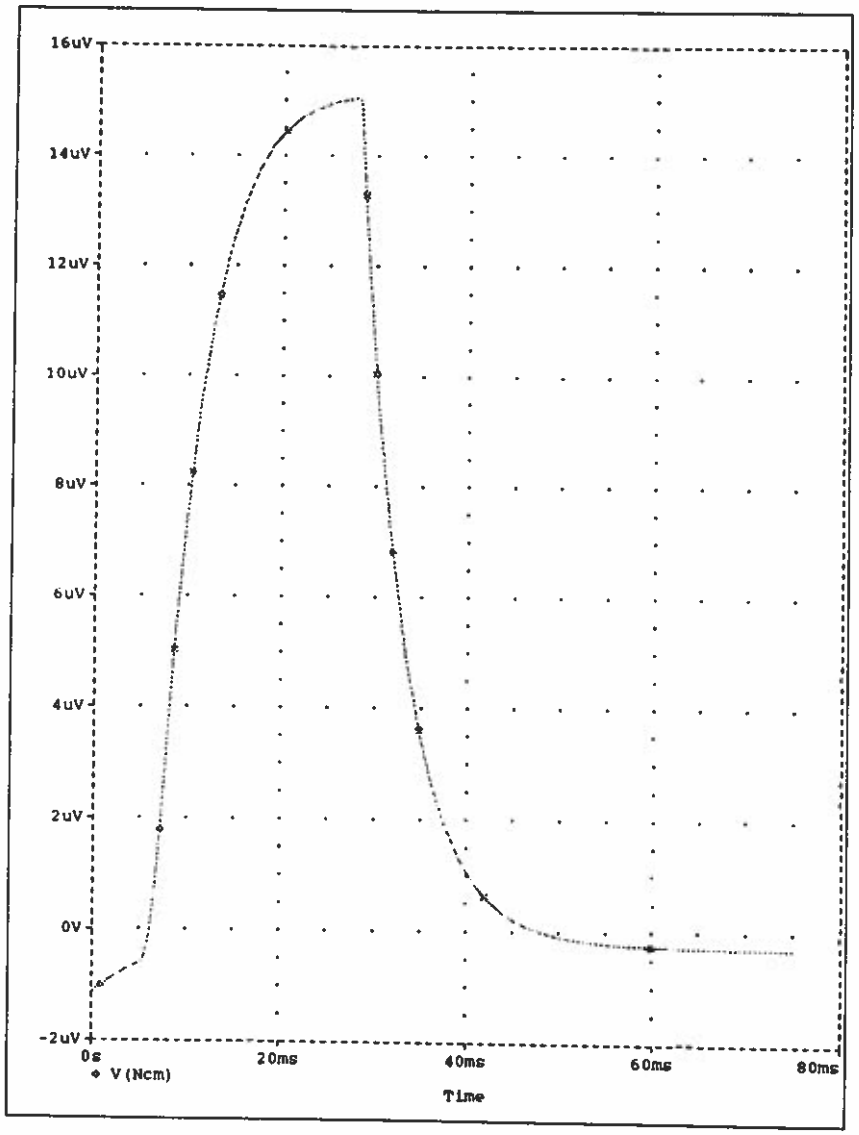

Fig. 5. The voltage V_{CM} across the capacitor C_M.

sodium channels. Although a large number of other sets can be used, the ones developed are of special interest since they should lead to transistor circuit realizations of the hair-cell-type circuits.

The semi-state equations derived present a number of difficulties for realization in terms of electronic hardware largely due to the fact that the equations include differential equations for conductance rather than for voltage and current. Consequently, a transfer of the equations into voltage and current ones was needed and that was carried out by numerically converting the conductances into voltages and then realizing the resulting currents via voltage controlled current sources (VCCS). It is in this direction that our equations have evolved. The best way to make a VCCS is usually to use a differential amplifier with a current mirror.[19] When BJTs are used this leads to an hyperbolic tangent gain function whereas when MOS transistors are used the result is a square root function, both of which can closely approximate the nonlinearities of (7) and (8).

State variable types of equations work with inputs and outputs while the equations of hair-cells are somewhat like resistors in that sometimes voltage is an input and sometimes current is an input, a property which one might call "non-orientedness." To reflect this non-orientedness of the hair-cell we developed two sets of canonical semi-state equations which will be useful for ear-type systems incorporating hair-cell types of behaviors.

Acknowledgements

The research of L. Sellami is partly supported by the Naval Academy Research Council. The authors wish to thank the reviewers for their constructive comments.

References

1. L. Sellami, "Kemp Echo Lattices Incorporating Hair-Cell nonlinearities," Doctoral Dissertation, Electrical Engineering, University of Maryland, 1992.
2. L. Sellami and R. W. Newcomb, "A Digital Model for Cochlea Characterization," *Proc. 5th Int. Conf. on Biomed. Eng.*, Santiago (Spain), Sept. 1994, pp. 15–16.
3. A. C. Crawford and R. Fettiplace, "The Mechanical Properties of Ciliary Bundles of Turtle Cochlear Hair-Cells," *J. of Physiol.*, **364**, Jan. 1985, pp. 359–379.
4. J. Howard and A. J. Hudspeth, "Compliance of the Hair Bundle Associated with Gating of Mechano-electrical Transduction Channels in the Bullfrog's Saccular Hair-Cell," *Neuron*, **1**, 1988, pp. 189–199.
5. G. A. Manley, *Peripheral Hearing Mechanisms in Reptiles and Birds*, Springer-Verlag, Berlin-Heidelberg, 1990.
6. C. J. Kros, "Physiology of Mammalian Cochlea Hair-Cells," Dallos, Popper and Fay Eds. "The Cochlea," Springer Handbook of Auditory Research, New York, 1996, pp. 318–385.
7. M. J. Hewit and R. Meddis, "An Evaluation of Eight Computer Models of Mammalian Inner Hair-Cell function," *J. Acoust. Soc. Am.*, **90**, No. 2, Aug. 1991, pp. 904–917.
8. S. Ross, "A Functional Model of the Hair-Cell - Primary Fiber Complex," *J. Acoust. Soc. Am.*, **99**, No. 4, April 1996, pp. 2221–2228.

9. D. C. Mountain and A. E. Hubbard, "Computational Analysis of Hair-Cell and Auditory Nerve Process," in *Auditory Computation*, Springer-Verlag, New York, 1996, pp. 121–156.
10. L. Sellami and R. W. Newcomb, "Synthesis of ARMA Filters by Real Lossless Digital Lattices," *IEEE Trans. Circ. and Sys. II*, **43**, No. 5, May 1996, pp. 379–386.
11. L. Sellami and R. W. Newcomb, "A Digital Scattering Model of the Cochlea," *IEEE Trans. Circ. and Sys. I*, **44**, No. 2, February 1997, pp. 174–180
12. D. T. Kemp, "Stimulated Acoustic Emissions from within the Human Auditory System," *J. Acoust. Soc. Am.*, **64**, No. 5, Nov. 1978, pp. 1386–1391.
13. T. F. Weiss, "Bidirectional Transduction in Vertebrate Hair-Cells: A Mechanism for Coupling Mechanical and Electrical Processes," *Hearing Research*, **7**, 1982, pp. 353–360.
14. T. F. Weiss and R. Leong, "A Model for Signal Transduction in an Ear Having Hair-Cells with Free-standing Stereocilia IV: Mechano-electric Transduction Stage," *Hearing Research*, **20**, 1985, pp. 175–195.
15. H. E. Secker, C. L. Searle, and T. A. Wilson, "Bidirectional Transduction by Hair-Cells," *J. Acoust. Soc. Am.*, **85**, 1989, pp. 2–13.
16. D. K. Hartline, *Synetsim 3.3 User's Manual*, Bekesy Laboratory, Honululu, HI, 1990.
17. R. W. Newcomb and B. Dziurla, "Some Circuits and Systems Applications of Semistate Theory," *Circ., Sys. and Sig. Proc.*, **8**, No. 3, 1989, pp. 235–260.
18. L. Sellami and R. W. Newcomb, "Semistate and Circuits for DRIVER Neural Network Modules," *Proc. 2nd Int. Symp. Singular and Implicit Systems*, Dallas, Dec. 1992, pp. 84–86.
19. R. L. Geiger, P. E. Allen, and N. R. Strader, *VLSI Design Techniques for Analog and Digital Circuits*, McGraw-Hill Publishing Co., NY, 1990.